# ERRORS DETERMINATION OF THE MEMS IMU

**Luu Manh Ha[1] , Tran Duc Tan[1], Nguyen Thang Long[1], Nguyen Dinh Duc[2], Nguyen Phu Thuy[1]**

[1] *Department of Electronics and Telecommunications, College of Technology, VNU*
[2] *Vietnam National University, Hanoi*

**Abstract.** The demand of navigation and guidance has been urgent for many years. In fact, INS is daily used in controlling flight dynamics. Nowadays, with the strong growth of Micro-Electro-Mechanical-System (MEMS) technology, the Inertial Navigation Systems (INS) is applied widely. However, there are existing errors in the accelerometer and gyroscope signals that cause unacceptable drifts. There are two kinds of noise in the INS: deterministic and stochastic errors. The deterministic noises are usually eliminated by the carefully calibration process but the stochastic noises are always difficult to treat.
In this paper, we have determined successfully the characteristics of the MEMS sensors' noise by analyzing the Power Spectrum Density (PSD) and the Allan variance of the experiment data. Combining these two methods will give us a reliable noise model that is applied directly to the Noise Eliminating Block (NEB).

## 1. Introduction

Nowadays, navigation and guidance are very important problems for marine, aeronautics and space technology. In such systems, Inertial Measurement Units (IMUs) are widely used as the core of the Inertial Navigation Systems (INS) [1]. In principle, an IMU consists of gyroscopes and accelerometers which measure angular velocities and accelerations in three dimensions. Recently, thank to the development of MEMS technology, the IMUs become smaller, cheaper and more precise. However, there are still problems with MEMS based the IMUs which are necessary to be solved. The position error of an INS increases rapidly with navigation due to the integration of measurement errors in the gyroscopes and accelerometers. In order to make the corrections, the errors are classified into *deterministic* errors and *stochastic* errors [2].

To eliminate the deterministic errors, we can specify them quantitatively by calibrating the device. It is, however, more complex in determination of the stochastic errors .An optimal filter such as Kalman one is often used. In this case, the parameters of those stochastic errors must necessary to be specified. In this paper, we have determined noise parameters of both deterministic and stochastic errors of MEMS based the IMUs. For the deterministic errors, a precise rate table has been used as a calibration device. For the stochastic errors, we have tried two different methods PSD and Allan variance. The PSD is known as a classical method to analyze signal, while Allan variance is a new method which can show more

information than the PSD. Combining these two methods will give us a reliable noise model that is applied directly to the Noise Eliminating Block (NEB).

## 2. Measurement and characterization

In this study, we used the MICRO-ISU BP3010 which consists of three ADXRS300 gyros and three heat compensated ADXL210E accelerometers [3]. The measurements are synthesized by IMU's micro-controllers and transmitted out via RS232 interface. The unit transmits output data as angular incremental and velocity incremental data in serial frames of 16 bytes at one of the user-selectable frequencies of 64 Hz, 32 Hz, 16 Hz or 8 Hz.

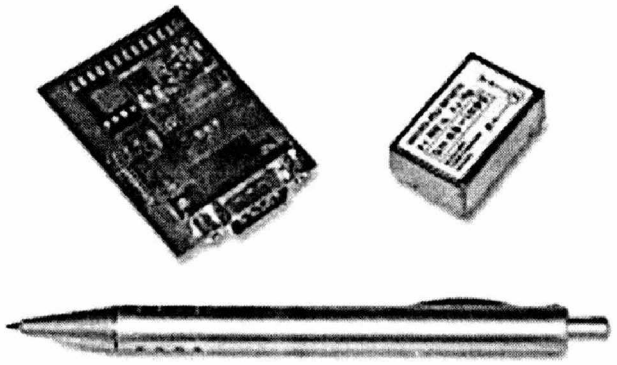

*Figure 1:* The MICRO-ISU BP3010 – A MEMS unit.

### *2.1 Deterministic errors*

Deterministic errors consist of bias, scale factor, inertial axis misalignment that are considered by the following error model [2]:

$$
\begin{aligned}
\delta a_x^b &= \alpha_x + \alpha_{xx} a_x^b + \alpha_{xy} a_y^b + \alpha_{xz} a_z^b \\
\delta a_y^b &= \alpha_y + \alpha_{yx} a_x^b + \alpha_{yy} a_y^b + \alpha_{yz} a_z^b \\
\delta a_z^b &= \alpha_z + \alpha_{zx} a_x^b + \alpha_{zy} a_y^b + \alpha_{zz} a_z^b \\
\delta \omega_x^b &= \beta_x + \beta_{xx} \omega_x^b + \beta_{xy} \omega_y^b + \beta_{xz} \omega_z^b + (\beta_{xyx} a_x^b + \beta_{xyy} a_y^b + \beta_{xyz} a_z^b)\omega_y^b + (\beta_{xzx} a_x^b + \beta_{xzy} a_y^b + \beta_{xzz} a_z^b)\omega_z^b \\
\delta \omega_y^b &= \beta_y + \beta_{yx} \omega_x^b + \beta_{yy} \omega_y^b + \beta_{yz} \omega_z^b + (\beta_{yxx} a_x^b + \beta_{yxy} a_y^b + \beta_{yxz} a_z^b)\omega_x^b + (\beta_{yzx} a_x^b + \beta_{yzy} a_y^b + \beta_{yzz} a_z^b)\omega_z^b \\
\delta \omega_z^b &= \beta_z + \beta_{zx} \omega_x^b + \beta_{zy} \omega_y^b + \beta_{zz} \omega_z^b + (\beta_{zxx} a_x^b + \beta_{zxy} a_y^b + \beta_{zyz} a_z^b)\omega_x^b + (\beta_{zyx} a_x^b + \beta_{zyy} a_y^b + \beta_{zyz} a_z^b)\omega_y^b
\end{aligned}
\tag{1}
$$

where $\delta a_i^b, \delta \omega_i^b$ ( $i = x, y, z$) are accelerometer and gyroscope errors expressed in the body frame.

$\alpha_i$ - Accelerometer biases [m/s$^2$].

$\alpha_{ii}$ - Accelerometer scale factor [unit less].

$\alpha_{ij}$ - Accelerometer installation error ($i \neq j$) [unit less].

$a_i^b$ - Accelerometer output in body frame coordinates [m/s$^2$].

$\beta_i$ - Gyro biases [rad/s].

$\beta_{ii}$ - Gyro scale factor [unit less].

$\beta_{ij}$ - Gyro installation error ($i \neq j$) [unit less].

$\beta_{ijk}$ - Gyro drift depending on acceleration, flexure error [m/s$^2$]

$\omega_i^b$ -Gyro output in body frame coordinates [rad/s].

In this paper, all installation errors and flexure errors will be neglected because they are very small. All of remaining deterministic errors are determined by the accelerometer and gyroscope calibrations.

*a) Accelerometer calibration*

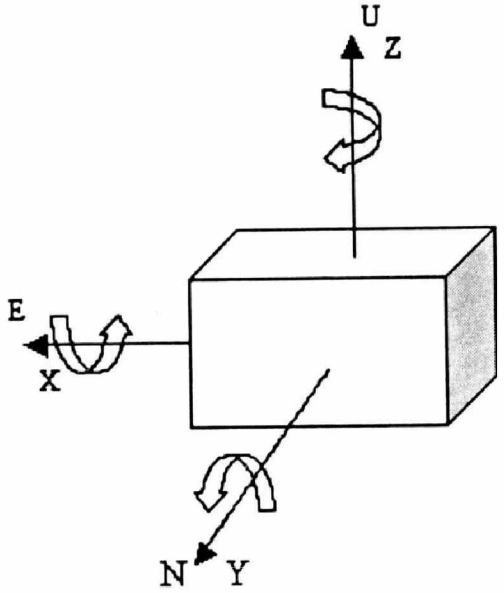


*Figure 2:* Initial IMU position for up-down calibration.

In the calibration procedure of the accelerometers, the earth gravity has been used. In this method, the IMU is initially positioned so that the Z-axis of the IMU aligned with the location level frames U-axis, the Y-axis of the IMU aligned with the N-axis and the X-axis aligned with the E-axis (Fig.2). It means that the gravity component will affect only the accelerometer along Z-axis by an amount of $+g$ ($g$ = 9.8 m/s$^2$). If the IMU is then rotated 180$^0$ around the Y-axis, a new measurement could be taken when the accelerometer along Z-axis senses the negative gravity ($-g$).

When the IMU with the $i^{th}$ accelerometer aligned with the U-axis in the navigation frame, the output of the accelerometer is:

$$z^1(a_i^b) = \alpha_i + (\alpha_{ii} + 1)g \tag{2}$$

Rotating the IMU 180$^c$ around perpendicular axis and making another measurement will give the following output of the accelerometer:

$$z^2(a_i^b) = \alpha_i - (\alpha_{ii} + 1)g \tag{3}$$

Solving set of equations (2) and (3) above, we can estimate of the accelerometer bias and scale factor:

$$\alpha_i = \frac{z^1(a_i^b) + z^2(a_i^b)}{2} \text{ and } \alpha_{ii} = \frac{z^1(a_i^b) - z^2(a_i^b)}{2g} - 1. \quad (4)$$

The collecting data process is performed for about 10 minutes for each position, then the data is averaged to give $z^1(a_x^b)$ and $z^2(a_x^b)$. Set of equations (4) is finally used to extract the accelerometer bias and scale factor. Calibration results showed that the accelerometer along Z-axis has bias of 0.1330 m/s$^2$ and scale factor of 0.0041.

*b) Gyroscope calibration*

The method is a calibration procedure that uses a precise rate table which contains sequence of different rates for each dimension has been made use. The IMU is initially positioned in center of rate table and each rate is run approximately for 10 minutes.

The error model equation of the gyro is:

$$w_{gi} = \beta_i + (\beta_{ii} + 1)(w_j + w_{ex}) \quad (5)$$

where $w_{gj}$ is nominal gyro angular rate at table angular rate $w_j$ [deg/h, rad/s].

$w_j$ . average table angular rate for data segment $j$ [deg/h, rad/s].

$w_{ex}$ . sensed component of earth rotation rate [deg/h, rad/s].

$\beta_i$ - gyro bias [deg/h, rad/s].

$\beta_{ii}$ - gyro scale factor.

From (5), we have:

$$\beta_{ii} = \frac{(w_{g1} - w_{g2}) - (w_1 - w_2)}{(w_1 - w_2)} \text{ and } \beta_i = \frac{w_{g1} + w_{g2}}{2} - (\beta_{ii} + 1)\frac{w_1 + w_2 + 2w_{ex}}{2} \quad (6)$$

We can then estimate gyro bias scale factor based on Eq.6. Results showed that the Z-axis gyro has bias of 0.3172 °/s and scale factor of -0.0070.

### *2.2 Stochastic IMU errors*

Some stochastic errors that affect the Initial Navigation Systems are listed as follows.

- *Quantization noise*

Quantization noise is made from encoding the analog signal into digital form. This noise is caused by the small difference between the actual amplitudes of the sampled signal and bit resolution of A-D Converter. We can reduce quantization noises by improving encode methods, adjusting sample rate, or increasing bit resolution.

- *White noise*

White noise can be a major source of the IMU errors and it has a constant power spectrum over whole frequency axis. Angle random walk (for gyroscope) and velocity random walk (for accelerometer) are caused by the white noise.

- *Random walk*

This is the random process of uncertain origin, possible of a limiting case of an exponentially correlated noise with long correlation time. The gyroscopes are affected by angular rate random walk, while the accelerometers are affected by acceleration random walk.

- *Flicker noise*

Flicker noise is low-frequency noise term that shows as bias fluctuations in data. This noise is caused by the electronics or other components that are susceptible to random flickering.

In order to analyze stochastic IMU errors, we have used the following methods:

*a) Power spectral density analysis*

The Power Spectral Density Analysis (PSD) describes how the power is allotted along the frequency axis [4]. The output data of the IMU, which is collected during an hour, is analyzed to give the PSD. Fig.3 shows a log-log plot of the PSD of the X-axis gyro. We note that there is a bunching of high frequency area. It is difficult to identify the noise terms and the parameters associated with them. Thus, the frequency averaging technique [5] has been used to smooth the PSD plot.

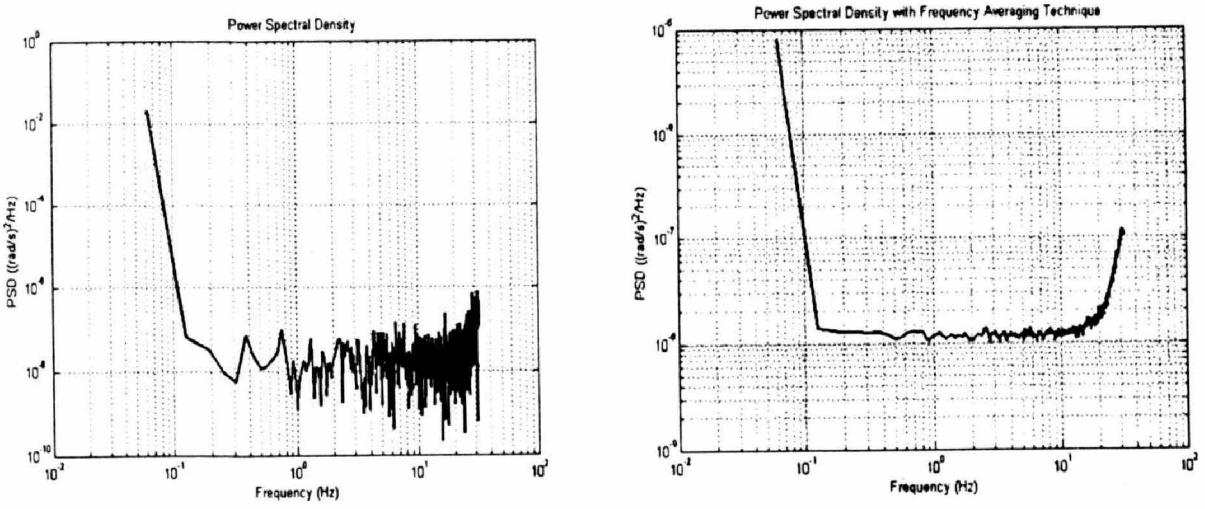


a b

*Figure 3.*The PSD plot of the X-axis gyro (a) and the PSD plot obtained by the frequency averaging technique (b)

Fig.3.b shows the PSD plot of the X-axis gyro obtained by the frequency averaging technique. The slopes of the curve comprise -2, 0 and 2. It means that the gyro data includes the angular rate random walk, the angle random walk and the quantization noise. The PSD of the X-axis gyro (see Fig. 3b) doesn't have the inclination of $-1$, which means that the Z-axis gyro lacks the angular rate flicker noise.

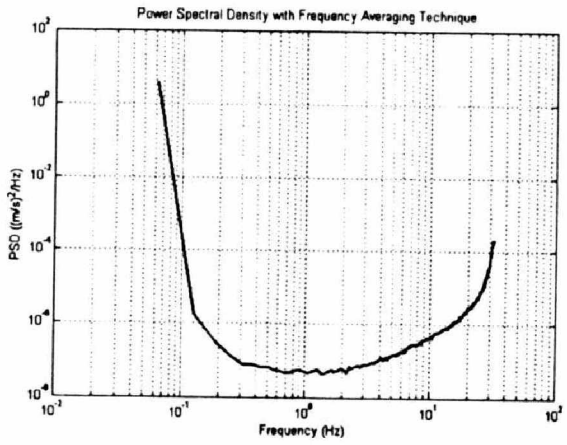


*Figure 4.* The PSD of accelerometer z obtained by frequency averaging technique.

Fig.4 shows the PSD plot of Z-axis accelerometer obtained by using the frequency averaging technique. The slopes of the curve comprise -2, -1, 0, 1 and 2. This curve indicates that accelerometer data includes acceleration random walk, acceleration flicker noise, velocity random walk, and acceleration quantization noise.

By using the converting formula in [6], we obtain from the PSD plot the angular rate white noise and the acceleration white noise as listed in Tab.1.

**Table 1.** Estimated white noise in the inertial sensors.

| Noise term | X | Y | Z |
|---|---|---|---|
| Angular rate white noise $^0/\sqrt{h}$ | 0,0560 | 0,0486 | 0,0578 |
| Acceleration white noise (m/s)/$\sqrt{h}$ | 0,0033 | 0,0030 | 0,0028 |

Analog Device states that angular random walk has values from 0 to $6^0/\sqrt{h}$ for the ADXLS300 gyros used in the MIRCO ISU BP3010 İMU. If we compare it to Table 1, we can see that the white noise level indeed lies within the limit of the manufacturer.

*b) Allan variance analysis*

The Allan variance is statistical measure to characterize the stability of a time-frequency system [7]. The PSD can only extract white noise standard deviation. In contrast, using the Allan variance, several other error parameters can be comprehensively derived.

The basic idea of the Allan variance is to take a long data sequence and divide it into segments based on an averaging time $\tau$ to process. Let give a sequence with N elements $y_k$, $k$= 0,1,..., *N-1*. Then, we define for each $n=1,2,3,...,M \leq N/2$ a new sequence of averages of subsequence with length $n$:

$$x_j(n) = \frac{y_{nj} + y_{nj+1} + \ldots + y_{nj+n-1}}{n}, \qquad j = 0,1,\ldots,\left[\frac{N}{n}\right] - 1 \tag{7}$$

If the sampling time is $\Delta t$, the time span within an averaged sequence of length $n$ is $\tau = n\Delta t$. The Allan variance, for a given subsequence length $n$, is defined as:

$$\sigma_a^2(\tau, N) \overset{\Delta}{=} \frac{1}{2\left(\left[\frac{N}{n}\right]-1\right)} \sum_{j=0}^{\left[\frac{N}{n}\right]-2} (x_{j+1}(n) - x_j(n))^2 \tag{8}$$

The typical slopes of the Allan variance for the gyroscope and the accelerometers in log-log plot are shown in Fig.6 with data collected from the IMU ISU BP3010 during an hour.

To determine the noise parameters, we need to fit the standard slopes in Fig 5 [8]. For example, if data contains white noise, the slope -1/2 will appear in the log-log plot of the Allan standard deviation.

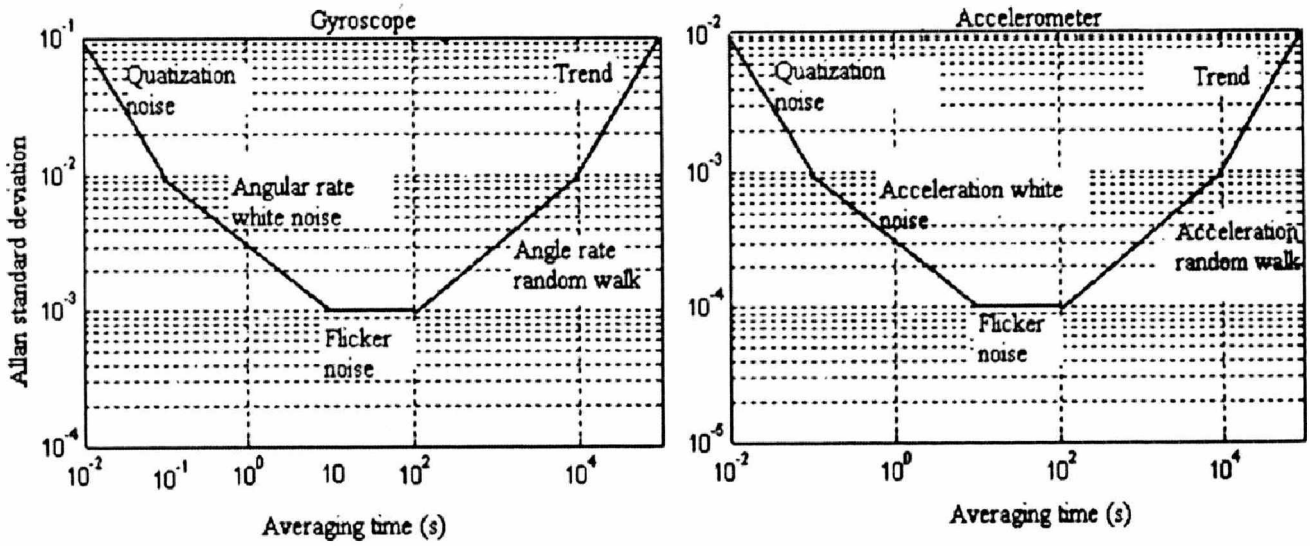


*Figure 5.* The standard slopes of the Allan standard deviation.

The log-log plot of the Allan standard deviation in Fig.6.a indicates the presence of angular rate quantization noise (slope -1), angular rate white noise (slope -1/2), angular rate random walk (slope 1/2), while angular rate flicker noise (slope 0) is absent. This result is fully consistent with that obtained by the PSD plot.

Figure 6b shows the log-log plot of the Allan standard deviation for the accelerometer. This shows the presence of accelerometer quantization noise (slope -1), accelerometer white noise (slope -1/2), accelerometer flicker noise (slope 0), and acceleration random walk (slope 1/2). This result is gain well consistent with that from the PSD plot. In addition, this shows the presence of acceleration trend (slope 1) that is unable to be indicated by only using the PSD plot.

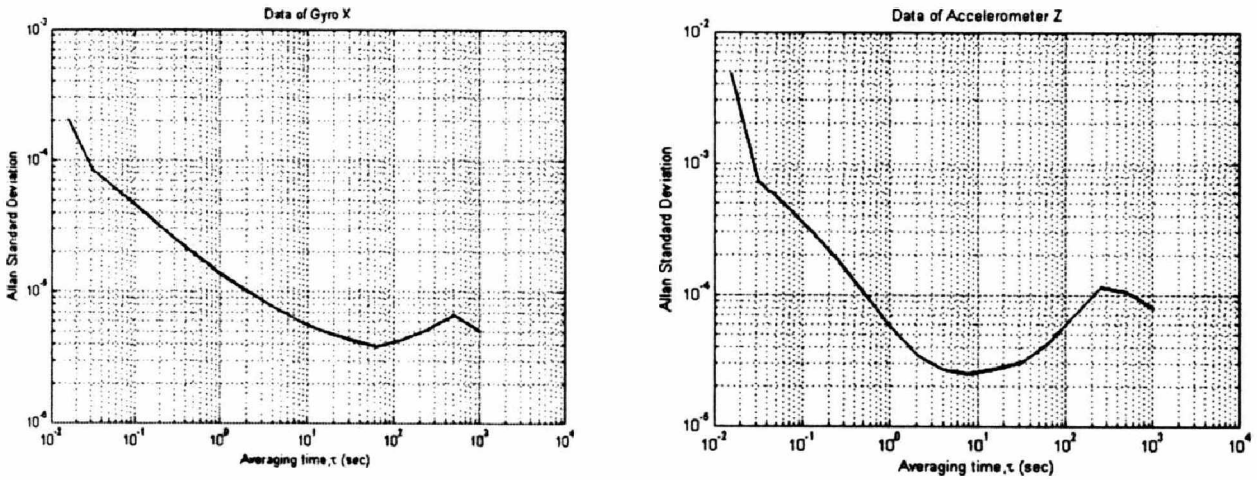


*a* *b*

*Figure 6.* The Allan standard deviation of gyro X (a) and of accelerometer Z (b)

The white noise coefficient is obtained by fitting the slope line at $\tau = 1$. Below the table shows the estimated noise coefficients for the gyros and the accelerometers.

**Table 2.** Identified Noise Coefficients, using Allan variance.

| Gyros | $Q_z$ (rad) (Quantization noise) | Q(rad/$\sqrt{s}$) (white noise) | B (rad/s) (Flicker noise) | K(rad/s/$\sqrt{s}$) (random walk) | R (rad/s$^2$) (trend) |
|---|---|---|---|---|---|
| X | 1,504*10$^{-6}$ | 1,368*10$^{-5}$ | X | 5,617*10$^{-7}$ | X |
| Y | 1,655*10$^{-6}$ | 1,517*10$^{-5}$ | 5,315*10$^{-6}$ | X | X |
| Z | 1,668*10$^{-6}$ | 1,535*10$^{-5}$ | 5,556*10$^{-6}$ | 4,892*10$^{-7}$ | X |
| | | | | | |
| Accelerometers | $Q_z$(m/s) | Q(m/s/$\sqrt{s}$) | B(m/s$^2$) | K (m/s$^2$/$\sqrt{s}$) | R(m/s$^3$) |
| x | 1,352*10$^{-5}$ | 4,734*10$^{-5}$ | 4,155*10$^{-5}$ | 1,161*10$^{-5}$ | X |
| y | 1,400*10$^{-5}$ | 5,169*10$^{-5}$ | 4,713*10$^{-5}$ | 7,588*10$^{-6}$ | 5.0685*10$^{-7}$ |
| z | 1,339*10$^{-5}$ | 5,688*10$^{-5}$ | 4,025*10$^{-5}$ | 9,197*10$^{-6}$ | 7.4025*10$^{-7}$ |

Character X means that the sensor lacks the error or this one is much smaller than the others.

*c) Comparison between PSD and Allan variance*

Table 3 shows the comparison between the PSD and Allan variance in extracting white noise coefficients. The results obtained by the two methods are much closed with each other which confirmed assert the reliability and the accuracy of the error model applied to the practical Inertial Navigation Systems.

**Table 3.** The comparison between the PSD and the Allan variance.

| | Gyros | | Accelerometers | |
|---|---|---|---|---|
| | PSD ([°/$\sqrt{h}$ ]) | Allan([°/$\sqrt{h}$ ]) | PSD([*m/s*/$\sqrt{h}$ ]) | Allan([*m/s*/$\sqrt{h}$ ]) |
| X | 0,0560 | 0.0470 | 0,0033 | 0,0028 |
| Y | 0,0486 | 0.0522 | 0,0030 | 0,0031 |
| Z | 0,0578 | 0.0528 | 0,0028 | 0.0026 |

## 3. Conclusion

This paper has succeeded in specifying the parameters of the IMU errors, which is a necessary step when applying error-processing algorithms for the INS. Estimation of the stochastic errors is more complicated than for the deterministic ones. Both of the two methods, PSD and Allan variance, have been used here to estimate the stochastic errors of the IMU. It is shown that the Allan variance is the more comprehensive method. The extracted results will be used as the parameters in Kalman filter for the INS-GPS integrated system.

**Acknowledgements.** This work is supported by the VNU program QGTD0509.

## References

1. Vikas Kumar N, *Integration of Inertial Navigation System and Global Positioning System Using Kalman Filtering*, M.Tech. Dissertation, Indian Institute of Technology, Bombay, July 2004.
2. Oleg S. Salychev, *Applied Inertial Navigation: Problems and Solutions,* BMSTU Press, Moscow Russia, 2004.
3. Georey J.Bulmer, *In MICRO-ISU BP3010 An OEM Miniature Hybrid 6 Degrees-Of-Freedom Inertial Sensor Unit. Gyro Symposium*, Stuttgart 16th-17th September, 2003.
4. Peter S. Maybeck, *Stochastic models, estimation, and control*, Academic Press, Vol. 1, 1994.
5. IEEE Std 1293-1998, Ieee standard specification format guide and test procedure for single –axis interferometric fiber optic gyros.
6. Wang, J., Lee, H.K., Rizos, C., *GPS/INS Integration : A Performance Sensitivity Analysis*, University of New South Wales, Sydney.
7. Haiying Hou, *Modeling inertial sensors errors using Allan variance*, UCEGE reports number 20201, Master's thesis, University of Calgary, September 2004.
8. Gyro, Accelerometer Panel of the IEEE Aerospace, and Electronic Systems Society. Draft recommended practice for inertial sensor test equipment instrumentation, data acquisition and analysis. In *IEEE Std Working Draft P1554/D14.*